15 Modeling of DME Engine Combustion Using Detailed Chemical Kinetics with Multidimensional CFD

Xiao Jin[1] Huang Zhen[1] Wang Xiaowu[2] Qiao Xinqi[1]
Shanghai JiaoTong University[1], Shanghai micropowers Ltd[2], P. R. China

Dimethyl ether (DME) has been recognized as a prospective alternative fuel for diesel engines because of its good characteristics of excellent auto-ignition quality, low flame temperature combustion and low emissions. In the present study, a model for DME injection process including the fuel injection system characteristics and its effect on spray characteristics is presented here. The model is validated with available experimental data. Detailed chemical kinetics was implemented in a multidimensional CFD code to study the combustion process in a diesel engine. The chemical mechanism of DME consisted of 31 species participating in 291 reversible reactions has been applied to simulation of DME spray combustion regime. The results of ignition delay, engine cylinder pressure, heat release and exhaust emissions have also been compared with experimental data and a good agreement has been demonstrated.

Keywords: DME, Engine simulation, Models

1. INTRODUCTION

There has been increasing research interest in alternative fuels for compression ignition (CI) engines as a consequence of legislation, or because the economics of certain areas of the world make these alternatives more attractive.[1-4] Lately, DME (Dimethyl ether, CH3OCH3), as an alternative fuel to meet the stringent future emission regulations and to reduce NOx, THC and PM from diesel engines, has attracted considerable attention because of its chemical properties - high vapor pressure, low viscosity, and high cetane number - that simultaneously minimizes the concentration and the amount of PM and NOx emitted from conventional CI engines. [5-6]

The objective of the present research was to better understand the performance and emissions characteristics of a four cylinder DI CI engine fueled with DME fuel using a three-dimensional CFD code with a detailed chemistry mechanism of DME for the ignition and combustion processes. The chemical mechanism of DME consisted of 31 species participating in 291 reversible reactions has been applied to simulation of DME spray combustion regime.[7] A model to simulated DME injection process including the fuel injection system characteristics and its effect on spray characteristics is incorporated into the three-dimensional CFD code. The numerical results of injection process, ignition delay, peak pressure, rate of pressure rise and heat release, and emission concentration profiles have been analyzed on the basis of physical and chemical characteristics of DME and have also been compared with the experimental results.

2. MODELS

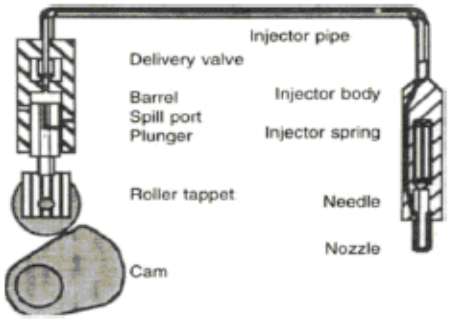

Fig.1 Schematic diagram of a pump-line-nozzle fuel injection system

The mathematical models developed or applied in the present study include models for the fluid flow through the fuel injection system chambers and high pressure pipes, models for the solid moving parts such as valves, and models for specifying important phenomena such as cavitation. Figure 1 shows a schematic diagram of a pump-line-nozzle fuel injection system. The system characteristics are summarized in Table 1.

Table 1. Pump-line-nozzle system dimensions

Plunger	Diameter	10 mm
	Stroke	11 mm
	Pressure in cam chamber	0.15 MPa
Delivery valve	Diameter	6mm
	Mass	5g
	Spring stiffness	7.171569 kg/ cm
High pressure pipe	Inner diameter	1.8mm
	Length	505mm
Needle valve	Mass	8.5g
	Max lift of needle	0.45mm
	Spring stiffness	135kg/cm
Sac chamber	Volume	0.24613cm^3
Nozzle	Number of spray holes	4
	Hole outlet diameter	0.55mm

The two main elements for fluid flow in this system are the pumping, delivery, nozzle, and sac chambers and the high pressure pipes. Models for specifying the fluid flow through the passages are required. In this case the mass conservation law is applied to the chambers, while the mass and momentum laws are used for the pipe flows. All the mathematical models are based on the following methods and assumptions:

1. A one-dimensional method is used for modeling the pipe flows. The flow properties are described at grid points, which are distributed throughout the fuel system. 2.Considering the possibility of the occurrence of cavitation, the fluid is assumed to be homogeneous at every node of the grid or within the chambers, and the fluid properties are specified in terms of pressure, density, velocity (for the pipe flows), and void fractions. 3. No heat transfer is considered, the temperature throughout the system is assumed to be constant. 4. The bulk modulus, K, is considered to vary linearly with pressure for the liquid phase, and is assumed to be a constant for the vapor phase. The equivalent bulk modulus for the homogeneous mixture at each node is specified as a function of the liquid and vapor moduli, and the void fraction. 5. The effect of elastic deformation on the sound speed in the thin-walled high pressure pipe is accounted for by the use of Young's bulk modulus; 5. The sound speed is a function of the fluid bulk modulus E and density ρ , and the wall bulk modulus E_1,

$$a=\sqrt{\frac{1}{\rho\{1/E+2/E_1\cdot[(D^2+d^2)/(D^2-d^2)+\mu]\}}}$$

A definition equation of the bulk modulus and an equation for the equivalent density of the homogeneous fluid provide a closed system for the solution of the three state variables, i.e., pressure, density, and void fraction. These two equations are represented as

$$\frac{d\rho}{\rho}=\frac{dp}{K} \tag{1}$$

$$\rho=\alpha\rho_v+(1-\alpha)\rho_l \tag{2}$$

The flow through the high-pressure passages is treated as a one-dimensional compressible flow with the following governing equations,

Momentum

$$\frac{\partial p}{\partial x}+\rho\frac{\partial U}{\partial t}+2\rho kU=0 \tag{3}$$

Mass continuity

$$\frac{\partial U}{\partial x}+\frac{1}{a^2\rho}\frac{\partial p}{\partial t}=0 \tag{4}$$

Here, k, is the flow damping coefficient in the pipe, and α is local velocity of sound.

This set of equations, coupled with Eq. (2), is solved for the pressure, density, velocity, and void fraction at each spatial grid node and time step.

Then equation (3) and (4) can be combined as a second-order partial differential equation,

$$\frac{\partial^2 U}{\partial x^2}-\frac{1}{a^2}\frac{\partial^2 U}{\partial t^2}-\frac{2k}{a^2}\frac{\partial U}{\partial t}=0$$

The method of the Finite Difference is applied for the solution of the partial differential equations for one-dimensional flow in the high-pressure pipes. Fig.2 shows the characteristics grid of the difference method.The velocity difference equatin is

$$U_{n+1,t+2}=m_aU_{n+1,t+1}+m_bU_{n,t}+m_cU_{n+2,t+1}-m_dU_{n+1,t}+m_eU_{n,t+1} \tag{5}$$

Where,

$$m_a,m_b=\frac{k\Delta t}{1+k\Delta t},\ m_c,m_d=\frac{1}{1+k\Delta t},\ m_e=\frac{1-k\Delta t}{1+k\Delta t}$$

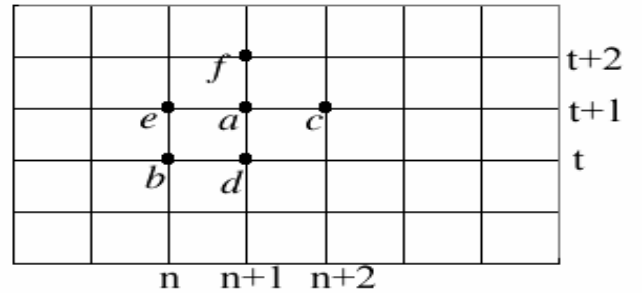

Fig.2 Schematic characteristics grid for the difference method

Then, the pressure at any time and any position in the high pressure line can be caculated by

$$p_{n+1,t} = p_{n,t} - a\rho(U_{n,t} - U_{n,t+1}) - 2\rho k\Delta L U_{n,t} \quad (6)$$

$$p_{n,t+1} = p_{n,t} + a\rho(U_{n,t+1} - U_{n+1,t+1}) \quad (7)$$

As vapor pressure of DME fuel being high, the internal nozzle flow is cavitating flow. The nozzle discharge coefficient, C_D, is defined as

$$C_D = \frac{\dot{m}_a}{\dot{m}_i} \quad (8)$$

where $\dot{m}_a$ and $\dot{m}_i$ represent the actual and ideal mass flow rates, respectively, which are expressed as

$$\dot{m}_a = A \cdot C_c \sqrt{2\rho\left(p_1 - p_v\right)} \quad (9)$$

$$\dot{m}_i = A\sqrt{2\rho\left(p_1 - p_B\right)} \quad (10)$$

where A is the passage cross-sectional area and Pv is the vapor pressure.

The effective velocity at nozzle exit is

$$u_e = \frac{2C_c p_1 - p_B + (1-2C_c)p_v}{C_c\sqrt{2\rho(p_1 - p_v)}} \quad (11)$$

The effective area at nozzle exit is

$$A_e = \frac{2C_c^2(p_1 - p_v)}{2C_c p_1 - p_B + (1-2C_c)p_v} A \quad (12)$$

In the simulation of fuel injection systems, the cylinder pressure is typically applied as the boundary condition for the fuel flow calculations. The engine cylinder pressure is not readily known at the equipment selection phase of the engine design. Moreover, this parameter is hard to quantify when modeling transient phenomena in the fuel injection system. The effect of the incorrect pressure boundary conditions on the accuracy of the injection rate predictions can be important, especially for lower injection pressure systems with maximum injection pressures around 700 bars. In the present methodology, the full 3-D CFD code was integrated within the pump-line-injector model.

The specifications and operating conditions of the diesel engine are listed in Table 2.

Cylinder bore (mm)	135
Stroke (mm)	140
Connecting rod length (mm)	280
Compression ratio	16.5
Number of Nozzle X diameter (mm)	4 X 0.55
Inlet air pressure (pa)	1. 03131E+05
Inlet air temperature (K)	320
Swirl ratio	2.3
Engine speed	1500rpm
Fuel	DME
Fuel injected	0.1632g/cycle

A detailed chemical kinetics mechanism of DME involving 291 reactions for 31 species has been used for simulating the ignition and combustion processes, which includes high temperature pyrolysis and oxidation, and low temperature oxidation (LTO) in the present study. The low temperature oxidation and high temperature oxidation (HTO) refer to those reactions occur below 800K and above 800K, respectively.[8-9]

The hybrid Kelvin-Helmholtz Raleigh-Taylor (KHRT) breakup model has been used to simulate the process of DME fuel injection.[10] The RNG k-ε model is used to simulated turbulence in diesel cylinder.[11] A characteristic time of combustion model has been used and extended to the present combustion modelling of DME study. The characteristic time scale for micro-mixing in the turbulence/chemistry interaction model is defined as

$$\tau_{characteristic} = \tau_{chem} + f \cdot \tau_{mix} \quad (13)$$

Where,

$$\tau_{mix} = \left(c_\mu / \mathrm{Re}_t\right)^{1/2} \frac{k}{\varepsilon}$$

$$f = \frac{1 - \exp(-r)}{1 - \exp(-1)}$$

*NO*X formation mechanism is considered in the coupled detailed chemistry of DME combustion and has the same essence of the extended Zeldovich mechanism. Since the soot emission is seldom found in diesel engines fueled with DME, no sub-model of the soot formation is considered in the present CFD simulation.

3.RESULTS AND DISCUSSIONS

The comparison of simulation results with experimental data is shown in Figs. 3 ,4 and 5. From these figures it is seen that the present pressure and needle lift simulation is in very good agreement with the measured data. However, there is a little discrepancy with the reflected wave, which is mainly due to a phase difference.

The time evolution of DME fuel concentration is shown in Figure 6. It shows that a liquid core exists near the nozzle, and the liquid jet penetration is not too far from the nozzle due to its lower injection pressure and the fast vaporization of DME fuel. Swirled air also promotes the fuel vaporization process

.The time profiles of simulated incylinder pressure is compared with experimental data, as shown in Figure 6. It shows that the agreement is excellent, which validate the PLN simulated model and the detailed chemical mechanism.

In the present diesel engine fueled with DME, the double peak of heat release rate profile cannot be observed in Figure 7. In the normal diesel engine, the first peak of heat release rate usually results from the premixed combustion. Since the diesel engine fueled with DME owes a shorter ignition delay and a milder premixed combustion, the peak heat release rate of premixed combustion disappears on the heat release rate curve and only the peak rate for diffusive combustion can be observed

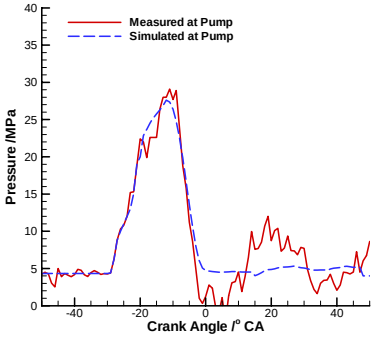

Fig. 3 Comparison the simulated results of pump pressure with experimental data

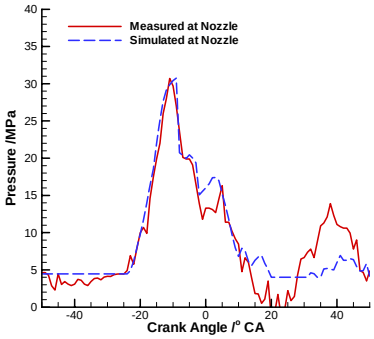

Fig. 4 Comparison the simulated results of nozzle pressure with experimental data

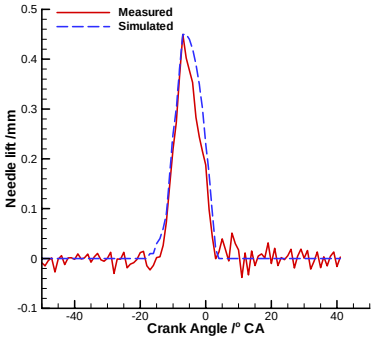

Fig. 5 Comparison the simulated results of valve lift with experimental data

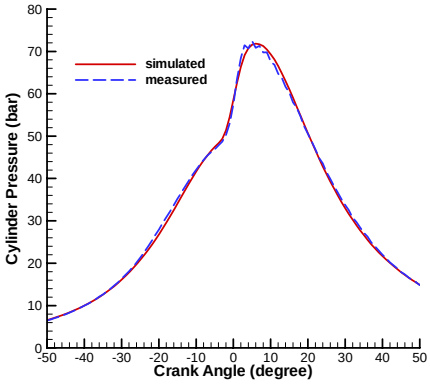

Fig.6 Comparison the simulated results of in-cylinder pressure with experimental data

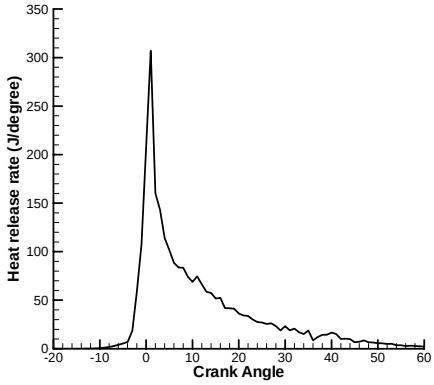

Fig.7 The simulated results of heat release rate

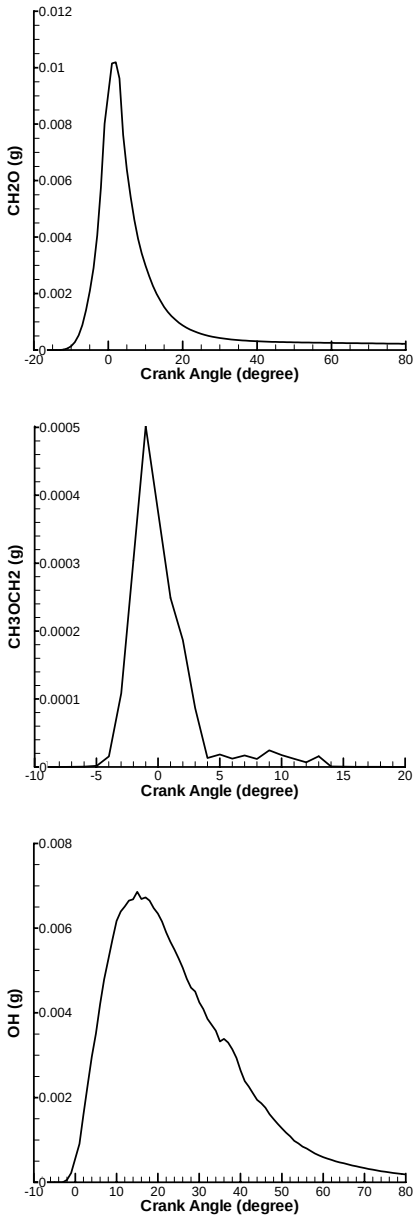

Fig.8 Simulated results of concentrations of *OH*, *C2H5O* and *CH2O* radicals versus crank angle.

In the present diesel engine fueled with DME, the double peak of heat release rate profile cannot be observed in Figure 7. In the normal diesel engine, the first peak of heat release rate usually results from the premixed combustion. Since the diesel engine fueled with DME owes a shorter ignition delay and a milder premixed combustion, the peak heat release rate of premixed combustion disappears on the heat release rate curve and only the peak rate for diffusive combustion can be observed.

As we known, the evolution of radicals plays a significant role in DME combustion. The concentration of radical *OH*, *CH3OCH2* and *CH2O* at different engine crank angles are shown in Figure 8. *OH* is the key radical and observed in all reaction active areas At low temperature condition, the molecule of DME reacts with radicals such as *OH* and forms *CH3OCH2* and leads to lower temperature oxidation. At high temperature condition, DME forms the methoxyl (*CH3O*) and methyl (CH3) radicals during the unimolecular decomposition, and the methoxymethyl (CH_3OCH_2) radicals proceed to the formaldehyde (CH_2O) and methyl radicals through β-scission. Therefore the concentration of CH_3OCH_2 can be rich in the temperature ranges from 900 to 1300K after LTO

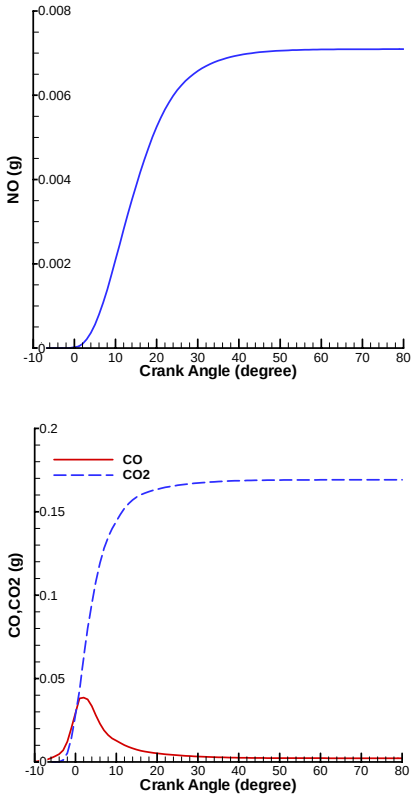

Fig.9 the emission of NO, CO and CO_2 simulated results .

Further increasing the temperature, the concentration of *CH3OCH2* will decompose and become lower in the high temperature areas. Similar trend is observed in *CH2O* radicals, which is the key intermediate stage during the start period of high temperature reactions.

Figure 9 show the NO, CO and CO_2 emission simulated results. The generation rate of *NO* rises at TDC and reaches to its maximum concentration at 50 CA ATDC steadily. The simulated *NOX* emission (a primary

composition is *NO*) has been determined to be 710 mg/m^3, which has a close agreement with the measured result of 682 mg/m^3. The time profile of *CO* and *CO*2 emissions shows that *CO* has a very low concentration and is only comparable to *CO*2 concentration at around 3 CA ATDC with its highest concentration 0.039g.

4. CONCLUSIONS

In the present study, a model for DME injection process including the fuel injection system characteristics and its effect on spray characteristics is presented here. Detailed chemical kinetics was implemented in a multidimensional CFD code to study the combustion process in a diesel engine. The results can be summarized as follow:

1. A fuel system simulation analysis methods for modeling the fuel injection system and nozzle internal flows have been developed and validated with available experimental data.
2. With the detailed chemical kinetics mechanism of DME fuel, the simulated results of in-cylinder pressure and heat release rate are better agreement with experimental data. Meanwhile, the simulated results of *NO*X and *CO*, CO_2 emissions agree well with the experimental data.
3. From the simulated results of our present study, the radicals such as OH, CH3OCH2 and CH2O play an important role in the oxidation reactions of DME which are in agreement with the earlier findings.

5. ACKNOWLEDGEMENT

This project was supported by National Natural Science Foundation of China (fund No.50136040) and National Key Fundamental Research Project of China (fund No.2001CB209208).

6. REFERENCES

1. H Fleisch and Peter C.Meurer, DME-The Diesel Fuel for the 21st Century _Presented at AVL Conference Engine and Environment 1995_ Graz, Austria

2. Theo Fleisch Chris McCarthy, Arun Basu _ Carl Udovich, Pat Charbonneau_Warren Slodowsked, Svend- Erik Mikkelsen, Jim McCandless, A New Clean Diesel Technology _ Demonstration of ULEV Emission on a Navistar Diesel Fueled with Dimethyl Ether. SAE 950061.

3. S.C.Sorenson, Svend-Erik Mikkelsen et al, Performance and emissions of a 0.273 Liter Direct Injection Diesel Engine Fuelled with Neat Dimethyl Ether, SAE Paper 950064.

4. Rasmus Christensen and S.C.Sorenson, Michael G.Jenser and Ken Friis Hansen et al, Engine operation on Dimethyl Ether in a Naturally Aspirated, DI Diesel Engine, SAE Paper 971665.

5. Ofner H., Gill D. W. and Krotscheck C., Dimethyl Ether as Fuel for CI Engines - A New Technology and its Environmental Potential. SAE Paper 981158.

6. Konno M., Kajitani S., Chen Z. L., Yoneda K., Matsui H. and Goto S., Investigation of the Combustion Process of a DI CI Engine Fueled with Dimethyl Ether. SAE Paper 2001-01-3504.

7. http://www.tfd.chalmers.se/~valeri/MECH.html

8. Fischer S.L., Dryer F.L. and Curran H.J. The Reaction Kinetics of Dimethyl Ether I: High Temperature Pyrolysis and Oxidation in Flow Reactors. International Journal of Chemical Kinetics, Vol. 32, 713-740, 2000.

9. Curran H.J., Fischer S.L. and Dryer, F.L., The Reaction Kinetics of Dimethyl Ether II: Low Temperature Oxidation in Flow Reactors. International Journal of Chemical Kinetics, Vol. 32, 741-759, 2000.

10.Reitz, R.D., Modeling Atomization Processes in High-Pressure Vaporization Sprays. Atomization and Spray Technology, Vol. 3, pp309-337, 1987

11. Kong, S.C., Han, Z. and Reitz, R.D., The Development and Application of a Diesel Ignition and Combustion Model for Multidimensional Engine Simulation. SAE Paper 950278.